Mechanical Testing and Diagnosis
ISSN 2247 – 9635, 2021 (XI), Volume 2, pp. 10-17

THE IMPACT OF DIFFERENT OUTWARD AND INWARD PROTRUSION POSITIONS ON THE NACA 1410 AIRFOIL SECTION AT VARIOUS ANGLES OF ATTACK

Raluca BALAȘA[1,2], Constantin Cristian ANDREI[2], Alexandru Gabriel ANDREI[1], Augustin SEMENESCU[1,3]

[1]Politehnica University of Bucharest, 313 Splaiul Independentei, 060032 Bucharest, Romania
[2]National Institute for Aerospace Research "Elie Carafoli" – INCAS Bucharest, Romania
[3]Academy of Romanian Scientists, Ilfov 3, 050044, Bucharest, Romania

E-mail: balasa.raluca@incas.ro

ABSTRACT

The current work aims to increase the NACA 1410 airfoil's aerodynamic efficiency by altering its surface qualities for various angles of attack. The NACA 1410 airfoil's lower surface has semicircular outward and inward protrusions for a more advantageous profile. The lift and drag coefficients were calculated using CFD, at various attack angles, from -2º to 18º. An ANSYS Fluent Workbench model of the NACA 1410 airfoil was used to investigate flow characteristics at 3 x 10^5 Reynolds numbers. The semicircular protrusions caused turbulence, reducing pressure drag and increasing lift, delaying flow separation. The NACA1410 profile has protrusions facing outward, increasing the pitch moment coefficient. The inward protrusion was found to be more advantageous in the study of the effects of surface alterations on airfoils at various angles of attack.

Keywords: NACA 1410, CFD simulation, outward protrusion, inward protrusion, low Reynolds number

1. INTRODUCTION

From the moment a new aircraft is under consideration, investments are made to improve aerodynamic efficiency as much as possible. The primary goal of any aviation expert or engineer is to make aircrafts more pilot-friendly, and significant efforts are being made to reduce drag. When it comes to increasing lift, flow separation is one of the most significant obstacles to overcome, and it can occur even at low speeds. When flow is moving at low subsonic speeds, it reattaches to the surrounding medium as a turbulent boundary layer [1]. When it comes to the design of small aerial vehicles, Mueller et al. [2] reported on the importance of Reynolds number and boundary layer effects on airfoils. The failure of laminar separation to reattach to the airfoil surface in time resulted in an abrupt decrease in lift and an abrupt increase in drag when the Reynolds number was low, as was observed. Zhang [3] is interested in the geometrical effects of airfoil flows on the separation and transition of the flows. Because of the rapidly varying surface curvature of the NACA 0012-64 airfoil, the DNS of incompressible flow over NACA 4412 and NACA-0012-64 airfoils revealed a stronger adverse pressure gradient field in the leading edge region of the NACA 0012-64 airfoil in the leading edge region. According to the above-mentioned literature, the poor aerodynamic efficiency of airfoils at high angles of attack in a low Reynolds number flow is caused by the separation of the flow streams in the flow. A large number of studies on the surface modification of airfoils have been conducted in order to improve the aerodynamic efficiency of the airfoil by delaying the separation of the flow streams. Diverse methods of delaying flow separation have been proposed by various researchers, for example, Zare Shahneh [4] that use vortex generators to create turbulence in order to defer boundary layer separation.

Using the standard NACA0015 airfoil, Siauw et al. [5] investigated the effects of impulsively activated pneumatic vortex generators. A statistical relationship between pressure and velocity signals during flow attachment and separations was established in this study at 100° angle of attack (AoA) for a Reynolds number of 1×10^6, and it described the flow regime and separation phenomenon. With respect to the NACA0012 airfoil, Niu et al. [6] investigated the dynamics of stalling and the effects of stalling on lift and pitching moment. A leading-edge technique with

variable droop was reported in the study, and it was found to reduce dynamic stall and improve aerodynamic characteristics. Improves in the aerodynamic performance of the NACA0012 airfoil, specifically an increase in the lift coefficient, have been observed with the introduction of a highly cambered flap. James et al. [7] proposed a method for controlling flow separation by secondary blowing, which resulted in increased lift and delayed stalling angles when compared to conventional methods.

A large number of experimental and numerical investigations on a wide range of airfoils have been conducted over the past decade to investigate their aerodynamic performance under a variety of boundary conditions. However, due to its compatibility with the user in analyzing flow characteristics, the use of analysis software has become significantly more popular. Matsson et al. [8] investigated the aerodynamic performance of the NACA 2412 with a chord length of 230mm when the Reynolds number was kept low. The stall angle was determined experimentally and through CFD simulations to be between 14º and 16º. In a steady state simulation with low subsonic flow of 50 m/s, Sarkar et al. [9] found that 50 AoA is optimal for the NACA 2412 airfoil model when using the NACA 2412 airfoil model. When applied to a NACA 2412 airfoil with a Reynolds number of 3 x 10^6, the numerical study compared the accuracy of Spalart Allmaras, k- ω SST, DES (Detached-Eddy Simulation), and k- ω SST turbulence models, and the results were conclusive. The results of the study show that DES k- ω SST is the most accurate method of simulating the flow over the NACA 2412 airfoil. Islam et al. [10] attempted to modify the NACA 2412 airfoil in order to increase the lift coefficient for low Reynolds number flow. They were unsuccessful. After increasing turbulence, the results showed that a sinusoidal leading edge, as well as an upper surface with protrusions that face outward, performs better. Dutta et al. [11] demonstrated that using flaps for different AoA for the NACA 2412 airfoil resulted in increased lift coefficients. However, it was discovered that at higher values of AoA, the lift coefficient decreased as a result of a decrease in the stall angle. Over the past few decades, surface modification with voids has proven to be a highly effective method of improving surface performance. Also because protrusions impart the necessary kinetic energy for reattachment of flow at low Reynolds number flow at higher angles of attack, the flow is reattached more frequently. Davies et al. [12] investigated the effect of voids on a golf ball and discovered that balls with shallower dimples produce longer drives, as their drag is reduced with a corresponding increase in the amount of lift produced. Later, Beves et al. [13] incorporated an array of protrusions into the airfoil and demonstrated that the velocity deficit in the wake was reduced to a minimum. At velocities of 30 m/s and 60m/s for AoA ranging from 50° to 250°, Livya and colleagues [14] investigated the effects of various-shaped protrusions, including semi-sphere, hexagon, cylinder, and square, on the NACA 0018 airfoil. The protrusion configuration with inward protrusions produced the best results, as it increased aerodynamic efficiency. Using the symmetric airfoil NACA 0018, Srivastav et al. [15] investigated the effect of inward and outward dimples and demonstrated that dimples are beneficial. Prasath et al. [16] conducted a CFD simulation for a NACA0018 airfoil with protrusions at a low subsonic velocity of 18 m/s using a computational fluid dynamics (CFD) model. The experimental results and the numerical simulations were in good agreement that the dimples cause delayed flow separation, which reduces the drag. After conducting an investigation into the effects of circular dimples on a NACA 2412 airfoil, Rajasai et al. [17] concluded that the presence of a circular dimple increases the stall angle of the aircraft. Devi et al. [18] investigated the effects of triangular and square cavities on a symmetric NACA 0012 airfoil design. The lift coefficient increased by 29.05% when the cavity was squared. A study conducted by Saraf et al. [19], examined a NACA0012 airfoil by varying the location of outer dimples and concluded that dimples at 75% of the chord length result in a 7% increase in lift coefficient. When Narayana et al. [20] investigated the flow parent for the NACA 4415 airfoil, they discovered that an inward protrusion at 0.8 along the chord and with a protrusion aspect ratio of 0.2 had the highest efficiency of all.

According to the literature [16], [17], [19], several attempts have been made to increase the lift of an airfoil by delaying the separation of the flow streams. However, no significant studies have been reported on the CFD analysis of a NACA 1410 airfoil with protrusions as a surface modification over wings when used as a surface modification over wings. The current research focuses on investigating the effects of surface modification on the aerodynamic performance of the NACA 1410 airfoil using computational fluid dynamics (CFD).

2. MODELING OF NACA 1410 AIRFOIL

In this study the surface parameters of the flow is simulated by the CFD in a 2D airfoil model, using the function dynamic mesh of ANSYS Fluent solver. The numerical model represents a CFD simulation of a 2D NACA 1410 airfoil model with the domain and a suitable grid mesh for every angles of attack (from -2° to 18°).

A stalling event in an airfoil is explained by Raymer [21] in terms of the thickness of the airfoil. It has been stated that a fat airfoil (with a thickness greater than 10 %) stalls from the leading edge, whereas thin airfoils stall from the trailing edge of the airfoil. Due to the fact that the NACA 1410 is a very thin airfoil, it stalls from the trailing edge. As a result, surface modification is supplied in the form of inner and outward protrusion, as well as an outer protrusion

of diameter 30 mm, located at a distance of 750 mm from the leading edge. The following table represents the model's wing specifications:

Table 1: Model wing specifications

Particulars	Characteristics
Airfoil series	NACA 1410
Chord	1000 mm
Protrusion type	Semi- circular
Protrusion diameter	30 mm
Protrusion location	750 mm chord (lower surface)

The grid independence test was performed in order to guarantee that the CFD simulations did not vary depending on the grid size. This procedure was used to determine the final number of nodes and grid size by going through several iterations. In order to get a 300000 nodes and about 600000 elements unstructured grid, the wall triangle approach was used to establish the grid's dimensions. In the non-dimensional cell wall distance parameter, or y^+, the distance from a wall to a specific cell height is defined as a function of the flow's parameters, such as cell height. Using a maximum y+ value of 0.2 in the analysis of airfoils, Eleni and colleagues [22] use a maximum y+ value of 0.7 in their analyses. Summary: According to Khare et al. [23], the value of y^+ must be less than 1, avoiding the need for wall functions, which "usually over anticipate the viscous drag in comparison." This is not practicable since it would be impossible to attain a first layer height y+ value of approximately one, especially while computing the answer while taking the larger velocity into account. The level of refinement would necessitate the use of resources that are in excess of what is now accessible. In ANSYS, you have the option of automatically refining your mesh. However, this would also be ineffective because the refinement would alter the mesh of each solution in a different way depending on the angle of attack. 1.68×10^{-5} mm should be the height of the initial cell, and the growth factor should be 1.08, with the non-dimensional cell wall distance parameter, or y^+, set to 1.

Table 2 shows the boundary conditions used for CFD study of airfoils with and without protrusions at various angles of attack from -2° to 18°. For example, in the inner region of the boundary layer, the solver uses the k-ω turbulence model. The first transported variable 'k' determines energy in turbulence. The second transported variable, specific dissipation, determines the turbulence scale. Menter [24] describes the SST k-ω turbulence model, which is a two-equation eddy-viscosity model that has gained widespread acceptance. It is possible to get the best of both worlds by using the shear stress transport (SST) formulation. By utilizing the SST k- ω model in the inner regions of the boundary layer, the model is directly usable all the way down to the wall through the viscous sub-layer, allowing the model to be utilized as a Low-Re turbulence model without the need for any additional damping functions to be included. In addition, the SST formulation flips to a k-ε behavior in the free-stream, avoiding the usual k- ω problem in which the model is overly sensitive to the turbulence features of the inlet free-stream turbulence. The SST k-ω model is commonly implemented because of its excellent performance in the presence of unfavorable pressure gradients and separate flows. In places with high normal strain, such as stationary regions and regions of rapid acceleration, the SST k-ω model produces turbulence levels that are a bit too high. The effect of this tendency on a normal k-ε model is, on the other hand, far less pronounced.

Table 2: Boundary conditions

Parameter	Condition
Flow velocity	44 m/s
Reynolds number	3×10^5
Y^+	1
Solver used	Pressure based
Fluid condition	Ideal fluid
Flow type	Unsteady
Viscous model	k- ω SST with standard wall function
Ambient temperature	300 K
Outlet pressure	0 Pa
Atmospheric pressure	1.01×10^5 Nm^{-2}
Wall condition	Stationary wall
Shear condition	No slip
Density	1.17 kg/m^3
Cp	1.005 KJ/KgK

3. RESULTS AND DISCUSSIONS

The results of simulations of NACA 1410 airfoils with and without surface modifications were compared at various angles of attack ranging from -2° to 18°. Computational fluid dynamics simulations of NACA 1410 airfoils with and without surface modifications were also performed. To achieve the best possible aerodynamic performance, the coefficient of lift (C_L), the coefficient of drag (C_d) and the coefficient of pitch (C_m) were determined and studied. Table 3 shows the outcomes of the CFD simulation as determined by the data collected.

With respect to angle of attack, Figure 1 depicts the relationship between lift coefficient and various positions of protrusion on the airfoil section. The cases under consideration include those with and without protrusions, as well as those with outward and inward protrusions. It has been noticed that an airfoil with no protrusion produces less lift. Protrusion causes the lift coefficient to steadily increase when the protrusion is introduced. As the angle of attack increases, the lift for both positions increases as well. When compared to a normal airfoil, the outward protrusion provides a significant drop in the lift reduction. When the angle of attack is 14º, the lift is first considerable and then gradually decreases.

Table 3: C_L, C_d, C_m for NACA 1410 airfoil with and without protrusions

Angle of attack	C_L	C_d	C_m	C_L	C_d	C_m	C_L	C_d	C_m
(α)	NACA 1410 airfoil without modifications			NACA 1410 airfoil with outward protrusion			NACA 1410 airfoil with inward protrusion		
-2	-0.11101	0.008937	-0.02435	-0.055518	0.016487	-0.02	-0.10761	0.009256	-0.024751
0	0.10818	0.00883	-0.02377	0.14156	0.015837	-0.016736	0.11204	0.00911	-0.024414
2	0.32645	0.009175	-0.02306	0.3419	0.015558	-0.014111	0.33156	0.009439	-0.024084
4	0.54255	0.009965	-0.02211	0.5435	0.015793	-0.0118	0.5482	0.010273	-0.023395
6	0.75412	0.01152	-0.02072	0.742	0.0167	-0.00921	0.75921	0.011758	-0.022073
8	0.95761	0.013245	-0.01843	0.93447	0.018465	-0.00614	0.96255	0.01412	-0.020051
10	1.1495	0.01622	-0.01513	1.1113	0.02156	-0.0015459	1.148	0.017795	-0.016163
12	1.3193	0.02067	-0.00991	1.2602	0.026602	0.0051465	1.303	0.023531	-0.0097613
14	1.4535	0.027588	-0.00279	1.3563	0.035837	0.012976	1.4029	0.033469	-0.0020874
16	1.5151	0.040441	0.003801	1.3373	0.05782	0.012593	1.3724	0.057577	-0.0031465
18	1.3976	0.074938	-0.00531	1.0774	0.11993	-0.017867	1.098	0.12207	-0.034415

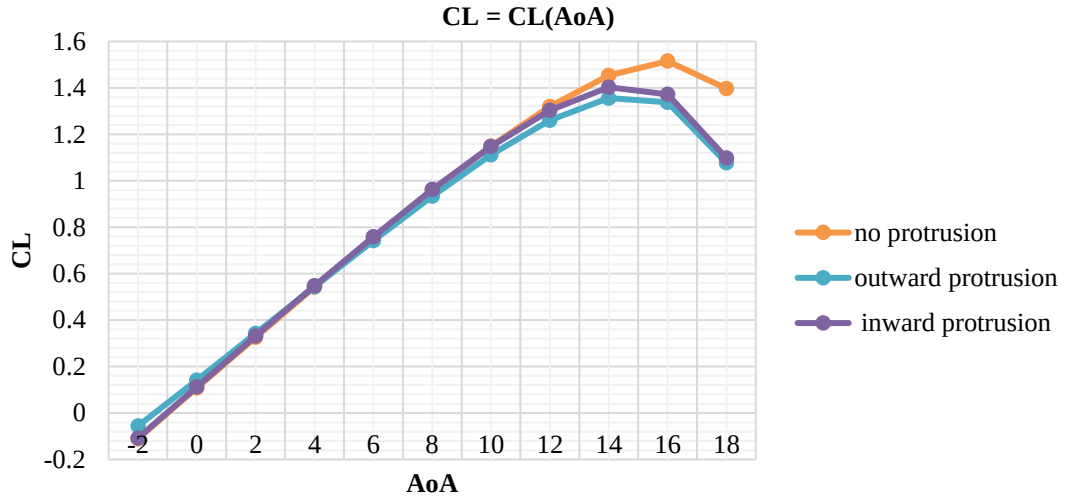

Fig. 1. Analysis Plot: CL versus AoA

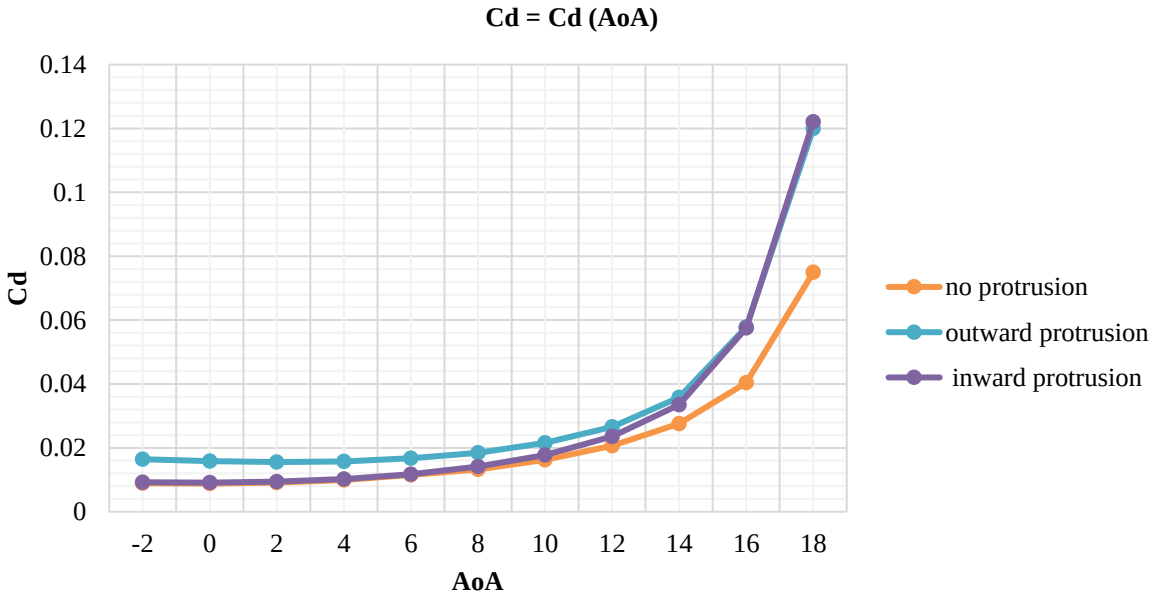

Fig. 2. Analysis Plot: Cd versus AoA

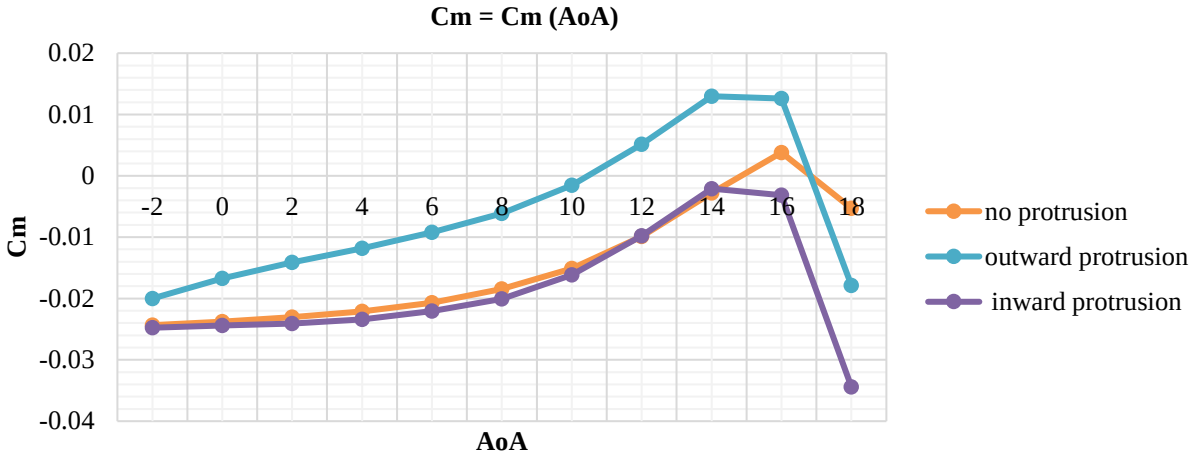

Fig. 3. Analysis Plot: Cm versus AoA

In Fig. 2, it can be observed that the inclusion of inward protrusion reduces the drag coefficient at low angles of attack up to an 8º angle of attack. The plain airfoil has the highest drag coefficient of all the airfoils. But the drag coefficient of a protruding airfoil at various places is much higher than for an airfoil without protrusion when compared to an airfoil without protrusion. Comparing the outward protrusion of an airfoil to that of a conventional airfoil, the drag has increased dramatically. When compared to the inward protrusion and standard airfoil, there is a decrease in the drag coefficient curve at 8º angle of attack; however, the curve grows as the angle of attack increases.

The pitch moment coefficient increases as a result of the shape of the NACA1410 profile, which features protrusions projecting outward, as seen in Fig. 3.

Air molecules move with the flow velocity under free-stream conditions; however, when the flow is halted by an airfoil, the molecules first impact its leading edge and their velocity decreases to zero. Figure 4 illustrates the 0° AoA NACA 1410 profile's pressure and velocity distributions.

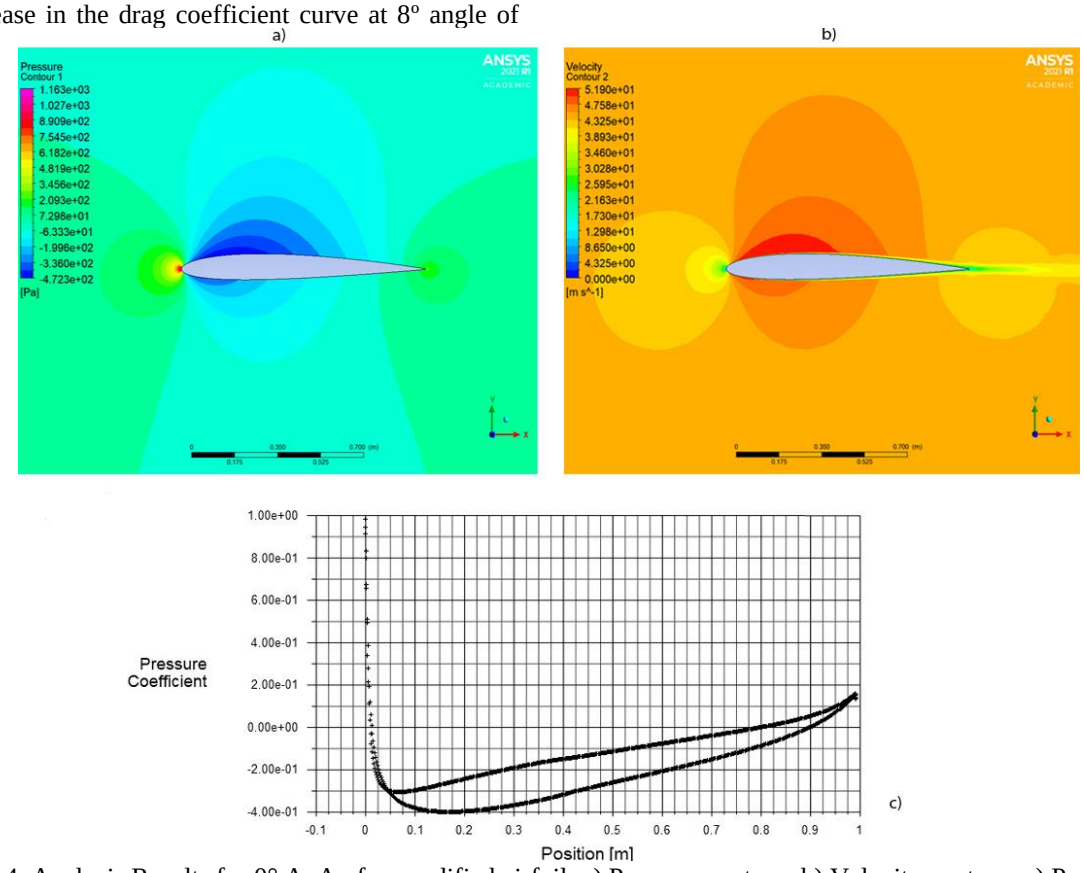

Fig. 4. Analysis Results for 0° AoA of unmodified airfoil: a) Pressure contour; b) Velocity contour; c) Pressure distribution along the length of the chord

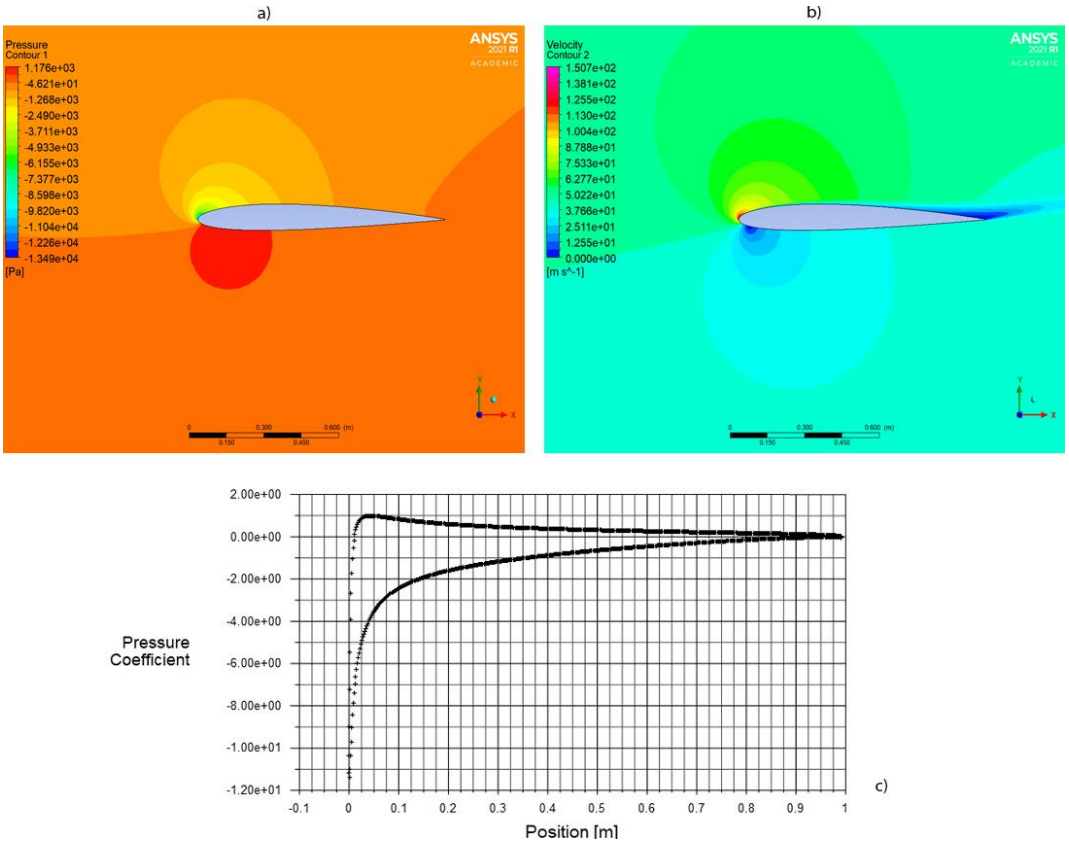

Fig. 5. Analysis Results for 14° AOA of unmodified airfoil: a) Pressure contour; b) Velocity contour; c) Pressure distribution along the length of the chord

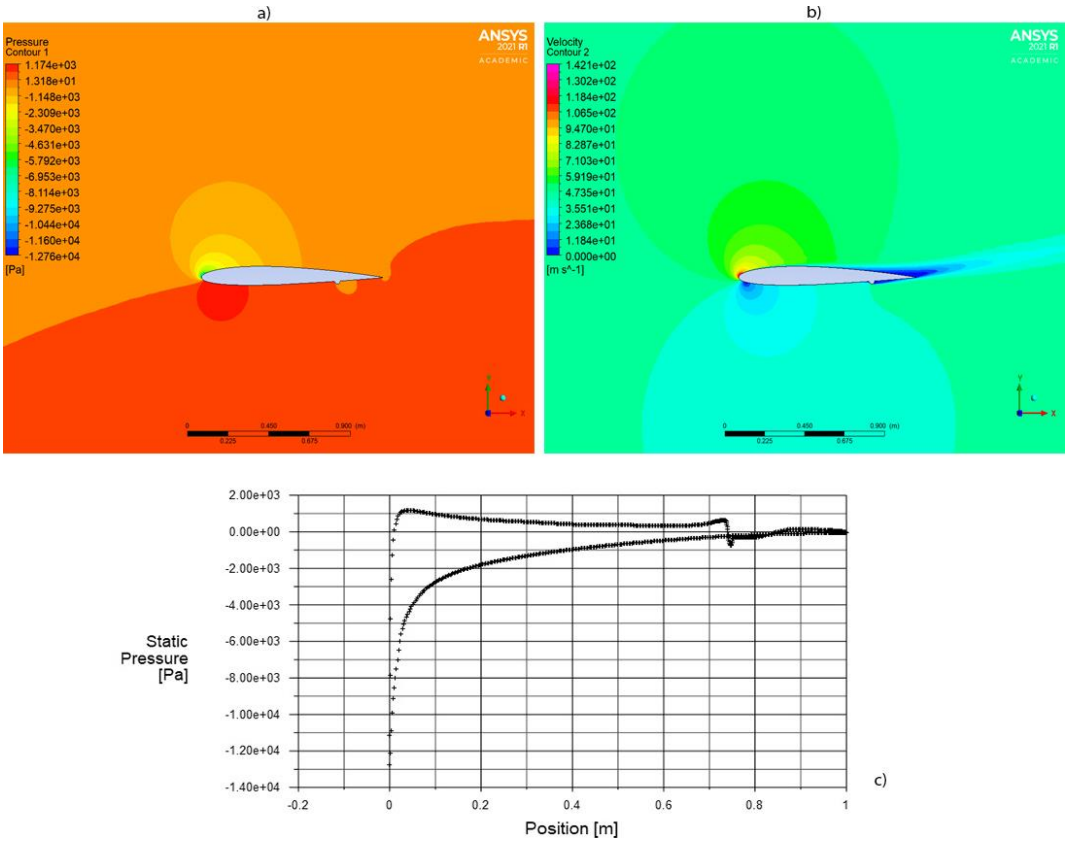

Fig. 6. Analysis Results for 14° AOA of airfoil with outward protrusion: a) Pressure contour; b) Velocity contour c) Pressure distribution along the length of the chord

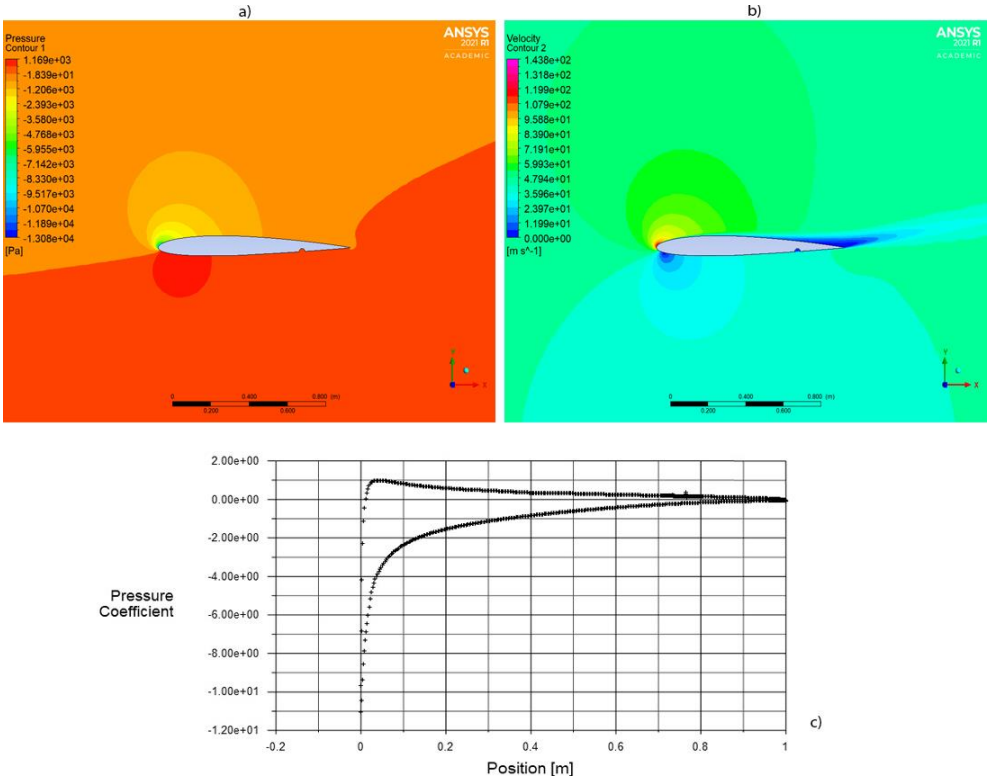

Fig. 7. Analysis Results for 14° AOA of airfoil with inward protrusion: a) Pressure contour; b) Velocity contour; c) Pressure distribution along the length of the chord

In order to increase the lift, the pressure on the upper surface should be lower than the pressure on the lower surface. The same can be observed clearly in the pressure contours depicted in Figures 5, 6 and 7. Higher AoA clearly shows that the flow separates from the trailing edge, which is quite noticeable. Having protrusions provides turbulent kinetic energy to the flow, which aids in reconnecting flow and, as a result, ensures that flow attaches to the airfoil surface when it occurs. Three separate conditions - outward protrusion, inward protrusion, and plain airfoil - are shown in the Figures 5b), 6b) and 7b) to illustrate varied velocity profiles at 14º angle of attack with three different conditions. It has been observed that the use of vortex generators causes boundary layer separation to be delayed, resulting in a reduction in pressure drag and an increase in the stall angle, respectively.

The outward protrusion has a significant impact on the flow, as can be seen in Fig. 6c), which represents the pressure distribution along the chord. Even from the simulation data, the drag coefficient and pitch coefficient of the outward protrusion have a wide range of values, which lead them to have a considerable impact on the flow.

The inward protrusion shown in Fig. 7 has greater aerodynamic qualities than the outward one. Because of this, it has been decided that the inner protrusion is more appropriate than the outward protrusion, as indicated by the findings of this study. The inward protrusion also gives greater aerodynamic efficiency.

4. CONCLUSIONS

Protrusions on a surface can improve the performance of an aircraft by altering the flow characteristics of the surface. A protrusion over a NACA 1410 airfoil has been shown to be more successful in adjusting lift, drag, and pitch forces than using a conventional airfoil. The following outcomes were obtained as a result of the work. First and foremost, the protrusions on the NACA1410 profile are oriented outward, enhancing the pitch moment coefficient.

The protrusion's curve also has the additional effect of accelerating the separation of the boundary layer, lowering the pressure coefficient and, when used in conjunction with the k-omega model, the shear stress limiter helps to prevent excessive turbulent kinetic energy accumulation at stagnation spots. Second, when the angle of attack (AoA) of the protrusion profile increases rapidly and the absence of a protrusion create a slight fluctuation in the profile, the pressure coefficient lowers, finally resulting in the formation of a small vortex in the profile.

The inward protrusion, as opposed to the other surface modifications, offers the finest aerodynamic qualities, as previously stated. It was found that the internal protrusion outperforms the outside protrusion in terms of aerodynamic efficiency and that the outer protrusion arrangement produces greater drag when compared to a standard airfoil. An inward protrusion will form over the airfoil, allowing for the observation

of boundary layer separation and protrusion, which will be arranged for the least amount of drag and maximum lift. It also improves the aerodynamic efficiency of the aircraft, which, in turn, improves its overall performance.

ACKNOWLEDGEMENT

This work is supported by the project **ANTREPRENORDOC**, in the framework of Human Resources Development Operational Programme 2014-2020, financed from the European Social Fund under the contract number 36355/23.05.2019 HRD OP /380/6/13 – SMIS Code: 123847.

REFERENCES

[1] Sowmyashree Y., Aishwarya D. I. P., Spurthy S., Sah R., Pratik B. V., Srikanth H. V., Suthan R., Study on effect of semi-circular dimple on aerodynamic characteristics of NACA 2412 airfoil, *AIP Conference Proceedings*, 2204, 030009, https://doi.org/10.1063/1.5141572, 2020.

[2] Mueller T. J., DeLaurier J. D., Aerodynamics of Small Vehicles, *Annual Review of Fluid Mechanics*, pp. 89-111, 2003, doi: 10.1146/annurev.fluid.35.101101.161102

[3]. Zhang W., Cheng W., Gao W., Qamar A., Samtaney R., Geometrical effects on the airfoil flow separation and Transition, *Computional Fluids*, **116**, pp 60-73, 2015.

[4] Shahneh A. Z., Computational analysis of tetrahedral vortex generator effect on the attenuation of shock induced separation, *International Journal of Applied Science and Technology*, **2(3),** pp. 34-52, 2012.

[5] Siauw W. L., Bonnet J. P., Transient phenomena in separation control over a NACA 0015 airfoil, *International Journal of Heat and Fluid Flow*, V. 67(Part B), pp 23-29, 2017, https://doi.org/10.1016/j.ijheatfluidflow.2017.03.008

[6] Niu J., Lei J., Lu T., Numerical research on the effect of variable droop leading-edge on oscillating NACA 0012 airfoil dynamic stall, *Aerospace Science and Technology*, **72**, pp. 476-485, 2018, https://doi.org/10.1016/j.ast.2017.11.030

[7]. Eldho S. J., Abhilash S., Jiss J. S., Abhay M., Kim H. D., Comparative study of boundary layer control around an ordinary airfoil and a high lift airfoil with secondary blowing, *Computional Fluids*, **164**, pp 50-63, 2017.

[8] Matsson J. E., McCain C. A., McGraw C., Aerodynamic performance of the NACA 2412 airfoil at low Reynolds number, *ASSE 23rd Annual Conference*, June 26-29 2016.

[9]. Sarkar S., Mughal S. B., CFD analysis of effect of variation in angle of attack over NACA 2412 airfoil through the shear stress transport turbulence model, *International Journal for Scientific Research & Development*, **5(2),** 2017.

[10] Islam T., Amit M. E. Arefin, M. H. Masud, Mourshedd M., The Effect of Reynolds number on the performance of a modified NACA 2412 airfoil, *International Conference on Mechanical Engineering AIP*; https://doi.org/10.1063/1.5044325.

[11]. Dutta P., Acharya A., Alam S., Bakaul S. R., Computational study on effect of flap deflection on NACA 2412 airfoil in subsonic flow, *Applied Mechanics and Materials*, **829**, pp. 9-14 doi: 10.4028/www.scientific.net/AMM.829.9.

[12]. Davies J. M., The aerodynamics of golf balls, *Journal of Applied Physics*, **20(9),** pp 821-828, 1949.

[13]. Beves C. C, Barber T. J., Aerofoil flow separation suppression using dimples, *The Aeronautical Journal*, **115(1168),** pp 335-344, 2011.

[14]. Livy E., Valli A.P., Aerodynamic analysis of dimpled effect on aircraft wing, International *Journal of Mechanical Aerospace Industrial Mechatronics and Manufacturing Engineering*, **9(2),** pp. 350-353, 2015.

[15]. Srivastav D., Flow Control over airfoils using different shaped dimples, IPCSIT, **33**, pp 92-97, 2012.

[16]. Prasath M. S, Irish Angelin S., Effect of Dimples on Aircraft Wing, *Global Research and Development Journal for Engineering*, 2(5), pp 234-242, 2017.

[17]. Rajasai B., Tej R., Srinath S., Aerodynamic effects of dimple on aircraft wings, *International Journal of Advanced Mechanical and Aerospace Engineering*, **2(2),** pp. 169-172, 2015.

[18]. Devi B., Shah D. A., Computational analysis of cavity effect over aircraft wing, *World Engineering & Applied Sciences Journal*, **8(2),** pp 104-110. 2017.

[19]. Saraf A. K., Singh M. P., Chouhan T. S., Effect of Dimple on Aerodynamic Behaviour of Airfoil, *International Journal of Engineering and Technology*, 2017, **9(3),** pp 2268-2277.

[20]. Narayana P. A. A., Rasya K. A., Prasad S. S., Effect of outward and inward dimple located on different positions of aerofoil section at a typical low Reynolds number, *International Journal of Engineering & Technology*, **7**, pp. 29-34, 2018.

[21]. Raymer D.P., *Aircraft Design: A Conceptual Approach*, Second Edition, American Institute of Aeronautics , 1992.

[22] Eleni D., Athanasios T., Dionissios M., Evaluation of the turbulence models for the simulation of the flow over a National Advisory Committee for Aeronautics (NACA) 0012 airfoil, *Mechanical Engineering Research*, **4(3),** pp. 100-111, 2012.

[23]. Khare A., Singh A., Nokam K., Best practices in grid generation for CFD applications using hypermesh, Computational Research Laboratories, 2009.

[24]. Menter F. R., Two-equation eddy-viscosity turbulence models for engineering applications, *AIAA Journal*, **32(8),** pp. 1598-1605, 1994.